Mem. S.A.It. Vol. 88, 298
© SAIt 2017
Memorie della

Supernovae from 8.8 and 9.5 solar mass stars: multicolor light curve simulations

A. Tolstov[1], S. Jones[2], K. Nomoto[1], and S. Blinnikov[3,4,1]

[1] Kavli Institute for the Physics and Mathematics of the Universe (WPI), The University of Tokyo Institutes for Advanced Study, The University of Tokyo, 5-1-5 Kashiwanoha, Kashiwa, Chiba 277-8583, Japan, e-mail: alexey.tolstov@ipmu.jp
[2] Heidelberg Institute for Theoretical Studies, Schloss-Wolfsbrunnenweg 35, D-69118 Heidelberg, Germany
[3] Institute for Theoretical and Experimental Physics (ITEP), 117218 Moscow, Russia
[4] All-Russia Research Institute of Automatics (VNIIA), 127055 Moscow, Russia

Abstract. Adopting the explosion properties derived by the first-principle simulations, we perform multigroup radiation hydrodynamics calculations of the light curves (LCs) for the massive electron capture supernova (SN) and the low-mass iron-core collapse SN. The simulations use evolutionary pre-SN models and derive multicolor LCs from shock breakout epoch to ^{56}Co decay, photospheric velocity and temperature evolution. The results of simulations constrain what observational features we can expect from low-mass SNe and help to distinguish types of their progenitors.

Key words. Stars: AGB and post-AGB – Supernovae: general

1. Introduction

The explosions of stars in mass range from 8 to 12 solar masses include both the most massive electron capture SN (EC-SN) and the lowest mass iron-core collapse SN (FeCCSN) (Nomoto 1984, 1987; Woosley & Heger 2015). Predicting the photometric and spectroscopic properties of these SN explosions is important to identify them in observations. But simulations of SN observational properties are often complicated by the lack of reliable pre-SN models. A step forward in construction of pre-SN models is stellar evolution simulations of Jones et al. (2013) to follow the most massive EC-SN progenitors to collapse, representing an evolutionary path to EC-SN in addition to that from super-AGB (SAGB) stars undergoing thermal pulses. The simulations also include the models through its entire thermal pulse phase until electron capture and models until the core-collapse. In this paper using several pre-SN models published by Jones et al. (2013) we overview the information that we can get from multicolor LC simulations. Here we limit our discussion by comparison of 8.8 $M_{\odot}$ and 9.5 $M_{\odot}$ models, while more complete study will be published elsewhere. The choice of these two models is due to their structure difference. While the 8.8 $M_{\odot}$ model possesses an SAGB-like structure following dredge-out, the 9.5 $M_{\odot}$ is more reminiscent of a massive star with distinct He- and C- shells.

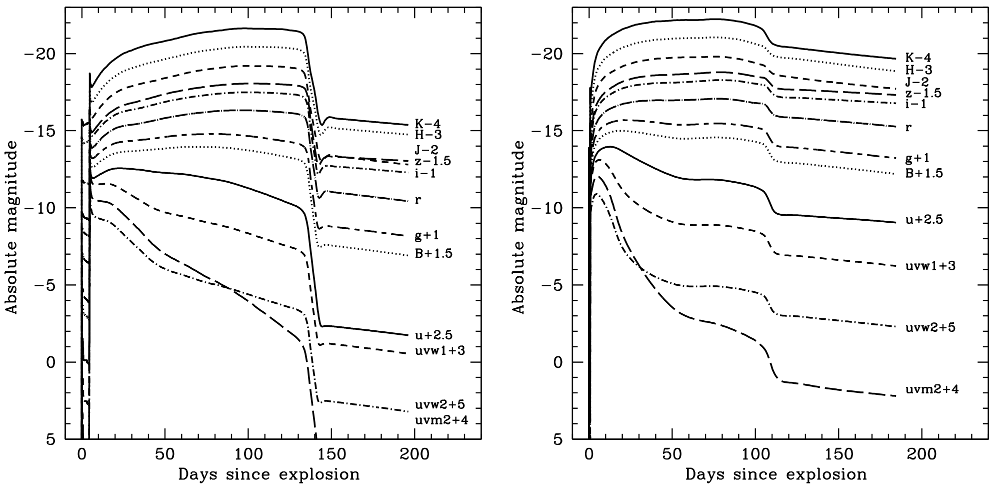

Fig. 1. Multicolor light curves in the models M880 (left panel) and M950E1 (right panel).

Table 1. Presupernova parameters

Model	M, $M_\odot$	Z, $Z_\odot$	$M_{\rm cut}$, $M_\odot$	lg R, $R_\odot$	$T_{\rm eff}$, 10^3 K	$M(^{56}\rm Ni)$, $M_\odot$	$E_{\rm kin}$, 10^{51} erg
M880	8.6	1	1.38	13.89	3.3	0.002	0.15
M950	9.3	1	1.50	13.48	4.2	0.002	0.15
M950E1	9.3	1	1.50	13.48	4.2	0.1	1

Note. The first column shows the model name. The numbers shown are the mass of the presupernova, the metallicity, the mass cut, the radius, the effective temperature, the mass of ^{56}Ni, the explosion energy.

2. Methods

We consider pre-SNe being red supergiant stars with extended H-rich envelope (Table 1). SN explosion energy and mass of the ^{56}Ni are parameterized by the most typical values for these types of SNe (Janka et al. 2008; Woosley & Janka 2005; Wanajo et al. 2013, 2017). Explosive nucleosynthesis should not affect the LCs significantly due to small ejecta mass from the core and it is not taken into account.

For calculations of the LCs, we use 1D multigroup radiation hydrodynamics numerical code STELLA (Blinnikov et al. 1998, 2000, 2006). The explosion is initialized as a thermal bomb just above the mass cut, producing a shock wave that propagates outward.

3. Results

3.1. Bolometric and multicolor light curves

The properties of SN LCs are determined by the structure and chemical composition of the progenitor. There are analytic estimations of the bolometric LCs (Litvinova & Nadezhin 1985; Popov 1993; Kasen & Woosley 2009), and based on the pre-SNe parameters it is easy to predict that the LCs of our models are plateau like with the duration of plateau phase

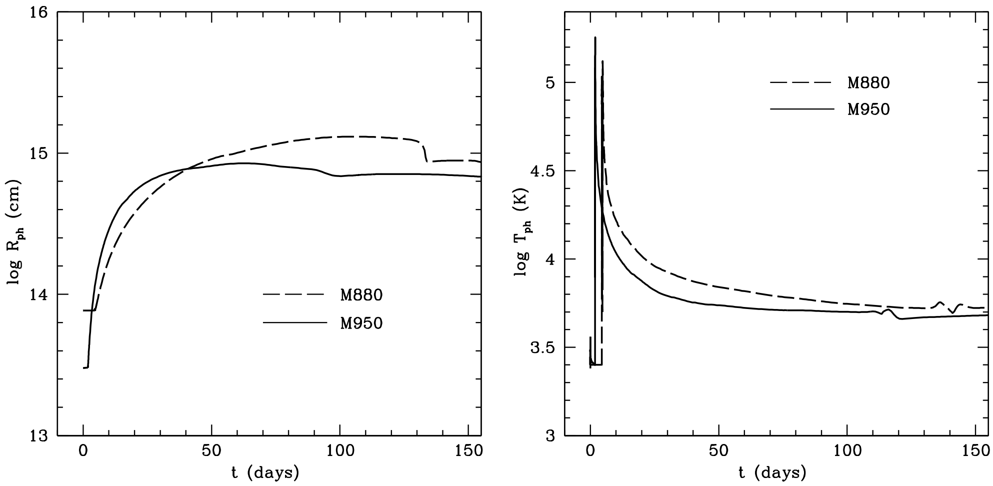

Fig. 2. Left panel: the comparison of the photosperic radius evolution in the models M880 and M950. Right panel: the color temperature evolution for the same models.

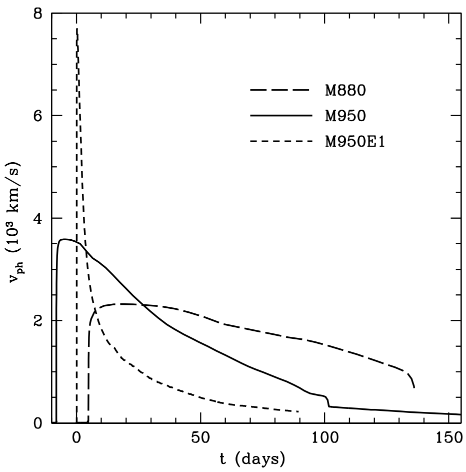

Fig. 3. Evolution of the photospheric velocities in the models M880, M950 and M950E1.

$t_{\rm p} \sim 100$ days and luminosity about $L_{\rm p,abs} \sim -15$. Thus, SNe are not faint due to large radius of their progenitors despite of low energy of the explosion.

More information we can get from multicolor LCs during plateau phase (Figure 1). In optical bands there is not so much difference in LC shape between M880 and M950 models, but bluer bands reveal faster decline of the LCs in more massive model, following the difference in structure of SN interiors.

3.2. Photosphere evolution

Larger density gradient of external layers of more massive model M950 leads to faster expansion of photosphere and faster decrease of the temperature in the beginning of the plateau phase (Figure 2). This is also the reason for higher velocity of photosphere in M950 model at the same explosion energy $E_{51} = E/10^{51}$ erg= 0.15 in the models M950 and M880 (Figure 3). In case of larger explosion energy $E_{51} = 1$ of FeCCSN velocity naturally increases.

3.3. Metallicity

We compare several progenitor models with similar density structure, but different metallicity ($Z = 0.014; 10^{-3}; 10^{-5}$). Bolometric LCs for these models do not have any low-metallicity specific features. The difference between the models is observed in U- and UV-bands where the luminosity decreases during plateau phase for solar metallicity model, while for the model with metallicity $Z = 10^{-5}$ the luminosity is close to constant during all plateau phase. This effect is discussed more in detail by Tolstov et al. (2017).

3.4. Comparison with observations

The rough comparison with observations (Pastorello et al. 2009) shows that bolometric LCs in mass range 8-12 $M_{\odot}$ fits several observed SNe (SN 1999em, SN 1999gi, SN 2003gd, SN 2004dj) with plateau luminosity $L_{\rm p,abs}$ from −15 to −16.5. Similar values of luminosity are also presented by Sukhbold et al. (2016) using different approach to calculation of SN LCs.

3.5. Mass loss

For SAGB stars at pre-SN epoch the mass loss rate can be rather high and the structure of the wind can also be complicated. In case of strong mass loss, the envelope with a mass less than several solar masses can explain low luminosity SNe. In case the envelope is completely lost our preliminary simulations produce low-luminosity LCs, that are similar to LCs produced by recently observed faint transients (Drout et al. 2014). An opposite situation we have in case of dense wind. The luminosity of the plateau phase increases up to $L_{\rm p,abs} \sim -19$ and it can be used to explain observed type IIn-P SNe (Chugai et al. 2004).

4. Conclusions

Our simulations show that intermediate mass stars produce plateau like SNe with typical duration of the plateau phase $t_{\rm p} \sim 100$ days. The LCs have a drop of luminosity after the plateau phase due to low amount of ^{56}Ni. Color evolution and photospheric velocities are defined by pre-SN structure and metallicity of the progenitor. The large uncertainty is mass loss. Depending on the rate it produces a wide range of LCs from faint SNe to rather luminous type IIn-P SNe.

In addition to construction of more realistic models, the multicolor LC observations from shock breakout to radioactive tail are highly in demand to clarify the late evolution of stars in intermediate mass range.

Acknowledgements. This research is supported by the World Premier International Research Center Initiative (WPI Initiative), MEXT, Japan, and JSPS KAKENHI Grant Numbers JP16K17658, JP26400222, JP16H02168, JP17K05382.

References

Blinnikov, S. I., et al. 1998, ApJ, 496, 454
Blinnikov, S., et al. 2000, ApJ, 532, 1132
Blinnikov, S. I., Röpke, F. K., Sorokina, E. I., et al. 2006, A&A, 453, 229
Chugai, N. N., Blinnikov, S. I., Cumming, R. J., et al. 2004, MNRAS, 352, 1213
Drout, M. R., Chornock, R., Soderberg, A. M., et al. 2014, ApJ, 794, 23
Janka, H.-T., et al. 2008, A&A, 485, 199
Jones, S., Hirschi, R., Nomoto, K., et al. 2013, ApJ, 772, 150
Kasen, D. & Woosley, S. E. 2009, ApJ, 703, 2205
Litvinova, I. Y. & Nadezhin, D. K. 1985, Soviet Astronomy Letters, 11, 145
Nomoto, K. 1984, ApJ, 277, 791
Nomoto, K. 1987, ApJ, 322, 206
Pastorello, A., Valenti, S., Zampieri, L., et al. 2009, MNRAS, 394, 2266
Popov, D. V. 1993, ApJ, 414, 712
Sukhbold, T., et al. 2016, ApJ, 821, 38
Tolstov, A., Nomoto, K., Blinnikov, S., et al. 2017, ApJ, 835, 266
Wanajo, S., Janka, H.-T., & Müller, B. 2013, ApJ, 767, L26
Wanajo, S., et al. 2017, arXiv:1701.06786 [astro-ph.HE]
Woosley, S. & Janka, T. 2005, Nature Physics, 1, 147
Woosley, S. E. & Heger, A. 2015, ApJ, 810, 34